Revista Geoaraguaia
ISSN:2236-9716
Barra do Garças – MT
v.10, n. esp. Geologia e Pedologia p.56-79. Dez-2020

A TYPOLOGY OF TEXTURES IN SOUTH NAGHADEH INTRUSIVE ROCKS, NORTHWESTERN IRAN

UMA TIPOLOGIA DE TEXTURAS EM ROCHAS INTRUSIVAS NO SUL DE NAGHADEH, NOROESTE DO IRÃ

Abdollah Kordi[1]

Afshin Ashja Ardalan*[2]

Seyed Jamal Sheikhzakariayi[3]

Nasser Ashrafi[4]

ABSTRACT

South Naghadeh is abundant in intrusive rocks. The region is part of Laramide magmatism in the Sanandaj–Sirjan zone and, from a petrological point of view, consists of syenogranite and monzogranite, granodiorite, quartz diorite, quartz monzodiorite, quartz monzonite, quartz syenite, and olivine gabbro. Available textures in local granitoid rocks include granular, granophyric, graphic, perthitic, and myrmekitic. The textures represent the formation conditions of the minerals, their layout in the rocks, and their physiochemical transformations during or after crystallization. The textures of local plutonic rocks (such as perthitic and granophyric) and lack of metasomatic aureoles and primary biotite are suggestive of high water vapor pressure and low emplacement depth of these rocks. The corona texture found in olivine gabbros was of the magmatic type.

Keywords: Intrusive Rocks; Texture Typology; Sanandaj–Sirjan Zone; Naghadeh; Iran.

RESUMO

Naghadeh do Sul é abundante em rochas intrusivas. A região faz parte do magmatismo de Laramide na zona Sanandaj – Sirjan e, do ponto de vista petrológico, consiste em sienogranito e monzogranito, granodiorito, diorito de quartzo, monzodiorito de quartzo, monzonita de quartzo, sienito de quartzo e gabro de olivina. As texturas disponíveis nas rochas granitóides locais incluem granular, granófico, gráfico, perthitic e mirmekitic. As

[1]Ph.D. Student in Petrology, North Tehran Branch, Islamic Azad University, Tehran, Iran. sam_habit2002@yahoo.com ORCID: http://orcid.org/0000-0003-3282-391X
[2]Assistant Professor, Department of Geology, North Tehran Branch, Islamic Azad University, Tehran, Iran *Corresponding author. afshinashjaardalan@yahoo.com ORCID: http://orcid.org/0000-0002-1800-9594
[3]Assistant Professor, Department of Geology, Science and Research Branch, Islamic Azad University, Tehran, Iran. j.sheikhzakaria@gmail.com ORCID.: http://orcid.org/0000-0002-4288-572X
[4]Assistant Professor, Department of Geology, Payame Noor University, Tehran, Iran. Nasser.ashrafi@gmail.com ORCID: http://orcid.org/0000-0003-2700-6560

texturas representam as condições de formação dos minerais, sua disposição nas rochas e suas transformações físico-químicas durante ou após a cristalização. As texturas das rochas plutônicas locais (como perthitic e granophyric) e a falta de auréolas metasomáticas e biotita primária são sugestivas de alta pressão de vapor de água e baixa profundidade de colocação dessas rochas. A textura corona encontrada nos gabros de olivina era do tipo magmático.
Palavras-chave: Rochas Intrusivas; Tipologia de Texturas; Zona Sanandaj – Sirjan; Naghadeh; Irã.

INTRODUCTION

Granitoid microstructures are classified into three main groups, namely magmatic, sub-magmatic, and solid-state (Blekinsop, 2000; Passchier *et al.*, 1998; 2005; Vernon, 2000, 2004). Further, granitoid rock textures are categorized into primary and secondary textures, with the former including granitic (granular), granophyric, graphic, and poikilitic textures, and the latter perthitic and myrmekitic textures. Myrmekite intergrowth is a solid-state microstructure for which several formation mechanisms have been proposed. This symplectic intergrowth occurs in plagioclase and vermicular quartz in massive and metamorphic granitoids, as well as metapelites, migmatites, aplites, and pegmatites (Menegon *et al.*, 2006; Mobashergermi *et al.*, 2018; Nazemi *et al.*, 2019). In the granophyric texture, quartz crystals grow in a branching (cuneiform-like) configuration out of an orthoclase matrix (Best and Christiansen, 2001; Vernon, 2004; Baratian *et al.*, 2018, Yazdi *et al.*, 2019a; 2019b, Zadmehr *et al.*, 2019). Graphic intergrowth is similar to but coarser than the granophyric type and contains more sodium or potassium-rich feldspar than intermediate compounds (Barker, 1970). Textural evidence shows, at most, two corona textures can form during magma solidification or under subsolidus conditions, which are referred to as magmatic corona and subsolidus corona, respectively. Sub-magmatic microstructures in granites include quartz, biotite, and chlorite-filled fractures in plagioclase phenocrysts. Undulose extinction of quartz with its surrounding recrystallized grains in granite rocks is considered a sub-magmatic–solid-state microstructure. Temperature rise and presence of fluids, particularly water, are highly significant in the formation of corona (Lang *et al.*, 2004).

GEOLOGY OF THE REGION

Located 7 km south of Naghadeh, 30 km east of Pianshahr, and 39 km west of Mahabad, the study region occupies 1200 sq. km. The area is located at 36°30’–37°00’ N and 45°15’–45°30’ E. This region is located east of the Naghadeh 1:100000 sheet (Figure 1). The oldest rock outcrops in the region include a collection of metasomatic rocks with greenschist facies and traces of igneous rock, forming the core of an anticline 10 km east of Naghadeh, along the Piranshahr road. The Cambrian deposits topping the said collection include Barut, Lalon, and Mila formations. Permian carbonate deposits were pushed above the said younger deposits by thrust faults. The large stratigraphic gaps date back to the Ordovician, Silurian, Devonian, and Carboniferous, while no trace of deposits from these periods is found in the region. That is all the while dolomites, and dolomite limestones of The Ruteh Formation from The Permian exhibit a wide spread, although, the bases of rocks from this period do not usually crop out. Cretaceous rocks are abundant in the area, spreading mainly across the southern parts of the study region. The Cretaceous sequence comprises green to gray shales and gray limestone. Based on the positioning of the upper and lower formations, the sequence belongs to a period from the Lower Cretaceous to the Late Cretaceous, but only evidence of the latter can be found in the study region. The broadest Cretaceous unit in the region is the one corresponding to the Late Cretaceous that holds shale and gray, slate, schist, and mica sandstones with pen erosion and thick and thin limestone strata in most areas.

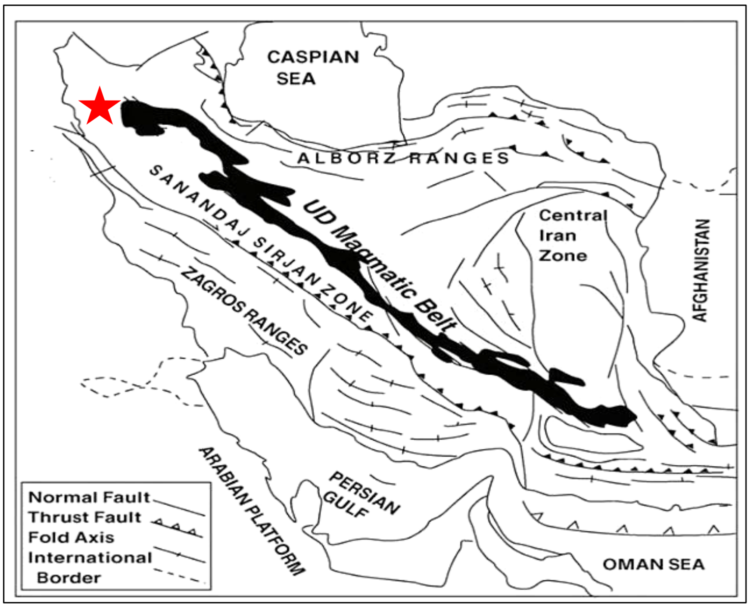

Figure 1. The study region in the structural zoning map of Iran.
Source: Gile *et al.* (2006)

PETROGRAPHY

Following extensive field investigations and thorough sampling of different petrological units of intrusive rocks, more than 130 microscope thin sections were prepared for investigation. After determining the quartz and alkali and plagioclase feldspars contents and bringing them up to scale for a sum of 100%, the Streckeisen diagram was used to name them (Figure 2).

Revista Geoaraguaia
ISSN:2236-9716
Barra do Garças – MT
v.10, n. esp. Geologia e Pedologia p.56-79. Dez-2020

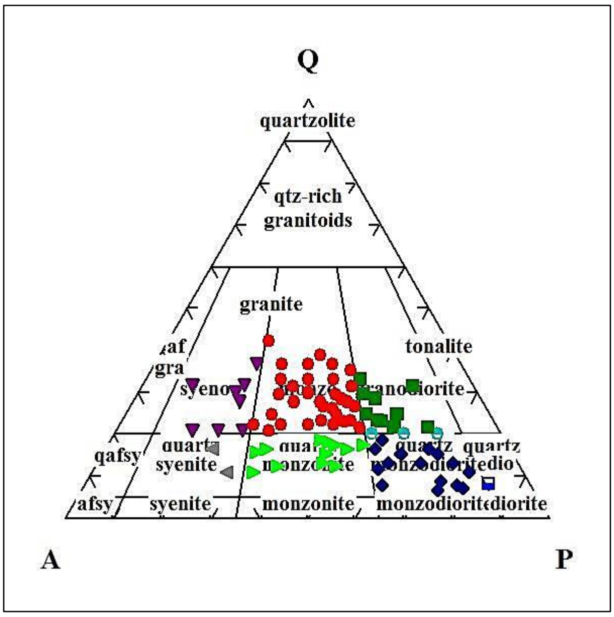

Figure 2. Typology of local intrusive rocks based on their modal compositions.
Source: Authors (2020).

<u>SYENOGRANITES AND MONZOGRANITES</u>

Granular, graphic, vein perthite, and secondary textures (resulting from alteration) are found in the specimens (Figure 3 a-f and Figure 4a-c), and plagioclase crystals have mostly become subautomorphic and sericitic. Carlsbad twinning and polysynthetic with oscillatory zoning exist in plagioclases, and chessboard (tartan) twinning is present in microclines. The essential mineral constituents, in order of abundance, are quartz (15–35%), potassium feldspar (20–45%), plagioclase (25–40%), and amphibole and its accessory minerals including sphene, zircon, apatite, biotite, and opaque minerals (primary and secondary) (Figs. 3a and b). Further, sericite, iron oxide (hematite), and chlorite can be mentioned as secondary minerals. The presence of microcline twinning in most orthoclase crystals can be suggestive of their solid-state metamorphism (Eggleton, 1979, Bouchez *et al.*, 1992; Eggleton, Buseck, 1980; Dabiri *et al.*, 2018). Orthoclase crystallizes in the monoclinic system, which changes to triclinic under stress. The switch in crystallization system from monoclinic to triclinic creates albite and pericline twinning in orthoclase (Fitzgerald, McLaren, 1982).

Revista Geoaraguaia
ISSN:2236-9716
Barra do Garças – MT
v.10, n. esp. Geologia e Pedologia p.56-79. Dez-2020

Most granites contain quartz crystals and two separately-grown feldspars, which is a consequence of gradual growth under equilibrium and high water pressure. That is, the high water pressure prevents the formation of a solid solution in alkali feldspars. However, near the surface, granites are substituted and crystallize quicker at a lower water pressure. Therefore, some solution forms in their alkali feldspars, leading to the crystallization of quartz and feldspar. With the volatile substances leaving, the liquidus and solidus curves rise and the cooling proceeds relatively rapidly. In this case, crystals do not spread separately and independently, but the simultaneous growth of quartz and alkali feldspar enables fine intergrowth. Fine intergrowth often takes place in existing phenocrysts resulting from slow cooling or pre-eutectic crystallization. The intergrowth takes the configuration of radial or branching quartz particles in a feldspar single-crystal (Shelley, 1993). In other words, with reduced water pressure, perthitic textures form in feldspars and fine grains between quartz and alkali feldspar.

GRANODIORITES

These rocks are less abundant than the others in the region. The light minerals of these rocks, including plagioclase (30–45%), quartz (10–25%), and potassium feldspar (10–30%) are scarce, and the accessory minerals include biotite, amphibole, sphene, and opaque. Chlorite, epidote, and sericite are secondary minerals, featuring subhedral granular (semi-formed grains), poikilitic, and graphic microtextures. Further, secondary textures also exist in these rocks due to alteration (Figure 3e).

QUARTZ MONZONITES

The granular texture is dominant in these rocks, but porphyritic, granophyric, and porphyritic also exist to some extent. The abundance of the plagioclase content was found to be 25–45%, alkali feldspar 50–50%, and quartz around 10–20%. Hornblende, at an abundance of 5–30%, and pyroxene, at 10–20%, are also found in the rocks. Apatite, sphene, and opaque minerals constitute the accessory minerals, whereas sericite, chlorite, epidote, and calcite are secondary minerals (Fig. 3e). In some plagioclases, the mineral transforms to sericite and epidote at the core but not on the edges, which can be attributed to the calcic nature of the mineral core, showing the regular zoning (Fig. 4a). Regular zoning is often suggestive of the slower rate of reaching equilibrium in the plagioclase system, relative to the crystallization rate. Given the fact that the Al/Si ratio regularly changes in the plagioclase, it does not react easily with lava (Shelley, 1993). Formation of zones in plagioclase can be due to two main reasons: a) plagioclase crystallization from a melt with shifting temperature, water vapor pressure, and composition (Humphreys *et al.*, 2006), and b) increased growth rate at the crystal–melt interface in response to equilibrium conditions (kinetic model) (Ginibre *et al.*, 2002a). In terms of dimensions, zones are classified into Coarse-Scale Oscillatory Zones (COZ) and Fine-Scale Oscillatory Zones (FOZ), and the former is the case with quartz monzonites.

In the shallow depth of the magma reservoir, magma is affected by dynamic activities, including convection or intrusion of hot, calcium-rich magma or both. Consequently, such textures as the fine sieve texture, zoning, and dissolution surfaces form separately around the rims of existing crystals (Singer *et al.* 1995). In the case of an extended arrest of crystal in the melt, a composition equilibrium is often established between plagioclase and magma without zoning. Zoning is indicative of a small rate of equilibrium compared to the rate of crystallization (Shelley, 1993). In some cases, alteration has taken place around or close to the edges of plagioclase (Fig. 4b). Most researchers, including Nixcon *et al.* (1987), turn to magma mixing, attributing the dissolved and reactive plagioclase edges to this phenomenon. Others, including Loomis (1982), on the other hand, raise volatile substances and oxygen fugacity variations in this regard.

QUARTZ SYENITES

Granular and poikilitic are the main textures in these rocks. Plagioclase content was found to be 20–25%, alkali feldspar 55%, and quartz around 10-15%. The hornblende content was also 10% with an approximate size range of 0.2–2 mm. Apatite, sphene, and opaque minerals constitute the accessory minerals, whereas sericite, chlorite, epidote, and calcite are secondary minerals.

QUARTZ MONZODIORITES

These rocks are holocrystalline with fine to average grains and contain hornblende and feldspar minerals. In microscope sections, the porphyritic, intergranular, and granular (average to coarse grains) textures are dominant, but the poikilitic texture is also found. Essential minerals include plagioclase (30–55%), alkali feldspar (10–30%), hornblende (15–20%), and quartz (under 10%). Accessory minerals include pyroxene, apatite, and opaque minerals, whereas sphene, chlorite, epidote, sericite, and clay minerals are secondary minerals (Figure 3e).

QUARTZ DIORITES

The most notable textures in local diorites are granular and microgranular and secondary textures resulting from deuteric alteration. Fine plagioclase crystals are found, on average, with an abundance of 45–55% in diorites and are in the labradorite range based on the extinction angle. Fine crystalline acicular microlites are scattered in the matrices of specimens with a porphyritic texture. At less than 10%, quartz fills the space between coarse plagioclase crystals. In some specimens, amphiboles contain opaque mineral inclusions and form a poikilitic texture. Augite is often found as a semi-formed to formed mineral, and secondary minerals include chlorite, epidote, sericite, and clay minerals. Some specimens contain 5–10% olivine.

OLIVINE GABBRO

These rocks often feature a granular to intergranular texture, as well as corona and poikilitic in some cases. The essential minerals in these rocks are plagioclase (40–55%), pyroxene (15–35%), and olivine (10–20%). The plagioclase composition is often of the anorthite type (40–55%) with sieve textures. Accessory minerals include apatite and opaque minerals, whereas chlorite, sericite, and clay minerals are the secondary minerals. Sieve textures form by either of two causes:

1. During pressure reduction processes (Nelson, Montana, 1992), the water-saturated magma rapidly rises to shallower depths, increasing the vapor pressure, reducing the stability of plagioclase crystals, and leading to the dissolution of crystals (Blundy, Cashman, 2005; Ashrafi *et al.*, 2018). The pits are then filled by melt and remain entrained in the crystal after recrystallization, forming the sieve texture. The sieve texture resulting from the process is coarse (Nelson, Montana, 1992). Steward and Pearce (2004) believe that the instabilities of the plagioclase crystals during the rapid ascent of magma creates the sieve texture. They attribute the outcome to the fact that the plagioclase melts partially, and the melting products crystallize within the crystal. Depending on whether the cooling rate is low or high, the products can crystallize in glass form or as secondary plagioclase in the initial plagioclase, creating the sieve texture.

2. Magma mixes or reacts with extremely hot, calcium-rich melt (Tsuchiyama, 1985). This mixing with the melt in the magma reservoir takes place at shallower depths, during which phenocrysts experience partial dissolution (Tsuchiyama, 1985). After partial dissolution, crystals react with the melt, reaching an equilibrium under the new conditions, and resulting in recrystallization. This process results in fine sieves, and studies show anorthite-rich plagioclase crystallizes at high temperature, under low pressure, and from a melt with high Ca/Na, Al/Si, and Ca/Al content and low water content (Nelson, Montana, 1992; Blundy, Cashman, 2005).

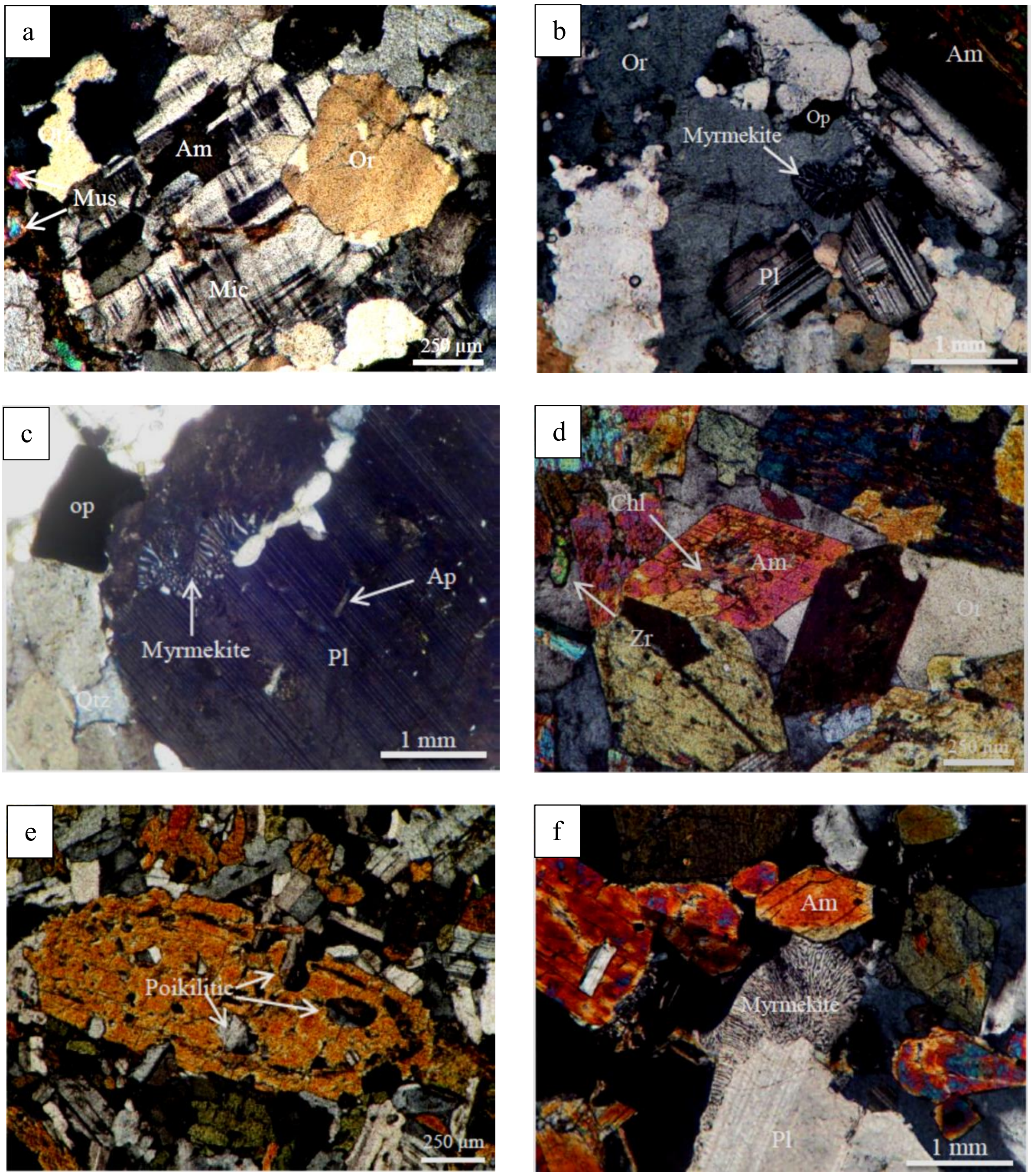

Figure 3. (*a*) a schematic of microcline with chessboard (tartan) twinning in monzogranite; (*b*) Granular and myrmekitic texture in monzogranite; (*c*) Granular and myrmekitic texture in syenogranite; (*d*) Granular and chloritized hornblende in syenogranite; (*e*) Granular and poikilitic textures in granodiorite; (*f*) Granular and myrmekitic textures in plagioclase in quartz monzonite.
Source: Authors (2020).

TEXTURE TYPOLOGY

Overall, the most notable textures found in local rocks can be classified into two groups.

a) Primary textures: Granular, granophyric, graphic, and poikilitic.

b) Secondary textures: Perthitic, myrmekitic, and corona.

a.1) Granitic Texture

This texture is the final stage of mineral cohesion and involves a mix of minerals of roughly the same sizes and shapes with planar, formed, and amorphous shapes joining together at the end of crystallization (Shelley, 1993) (Figure 3a).

a.2) Granophyric Texture

The texture is the result of the simultaneous and irregular growth of quartz and orthoclase (Figure 4b). In the texture, quartz crystals grow in a branching (cuneiform-like) configuration out of an orthoclase matrix (Best, Christiansen, 2001; Vernon, 2004). In this texture, relatively euhedral alkali feldspar crystals grow in a thick granite melt, and as the melt is enriched with silica and alkali elements, quartz–feldspar intergrowth develops around them (Best, Christiansen, 2001;).

Quartz is mostly dendritic in this texture and forms at—relatively—low temperature (around 650 °C), when the water content of magma is low due to rapid nucleation (Vernon, 2004; Tarabi *et al.*, 2019).

Different theories have been proposed regarding the formation of this texture. Vogt (1930) and Smith (1974) attribute the granophyric texture to the cotectic crystallization of quartz and alkali feldspar. In other words, the said texture is a primary texture in granitoid rocks that has solidified in a shallow depth (Best, Christiansen, 2001; Vernon, 2004; Dunhum, 1965; Hughes, 2003; Gholizadeh *et al.*, 2016; Yazdi *et al.*, 2017). The texture can be a product of subsolvus magma crystallization in the Qz-Ab-Or system on the cotectic line. Put differently, the high content of liquids is the reason for such intergrowth (Shelley, 1993). The formation mechanism of the granophyric texture is explained by feldspar nucleation as temperature decreases. The initial growth of feldspar creates a fluid supersaturated with silica and rich in H2O. In the process, skeletal feldspar forms and quartz fills the spaces between feldspars (Shelley, 1993).

a.3) Graphic Texture

Graphic intergrowth is similar to the granophyric type. The denomination of this texture is inspired by the resemblance of intertwined quartz branches to hieroglyphs or cuneiform symbols. Graphic intergrowth is coarser than granophyric and contains more sodium or potassium-rich feldspar than intermediate compounds (Barker, 1970). The intergrowth is often found in granite pegmatites and forms when liquids are present in ample quantities. However, it can also be the result of primary feldspar crystallization and the kinetic effect of the growth process on the system (Fenn, 1974) (Figure 4c).

a.4) Poikilitic Texture

The poikilitic texture was found in the rocks of the study region. Given the presence of hydrous minerals in the area, the water vapor pressure and the rapid pressure drop have contributed to the formation of the poikilitic texture. Magma mixing (Tsuchiyama, 1985) and liquid intrusion into the magma reservoir in large quantities are also effective in the formation of this texture. According to Hogan and Gilbert (1995), the poikilitic texture in minerals is the result of an adiabatic pressure drop in the magma (Figure 4d).

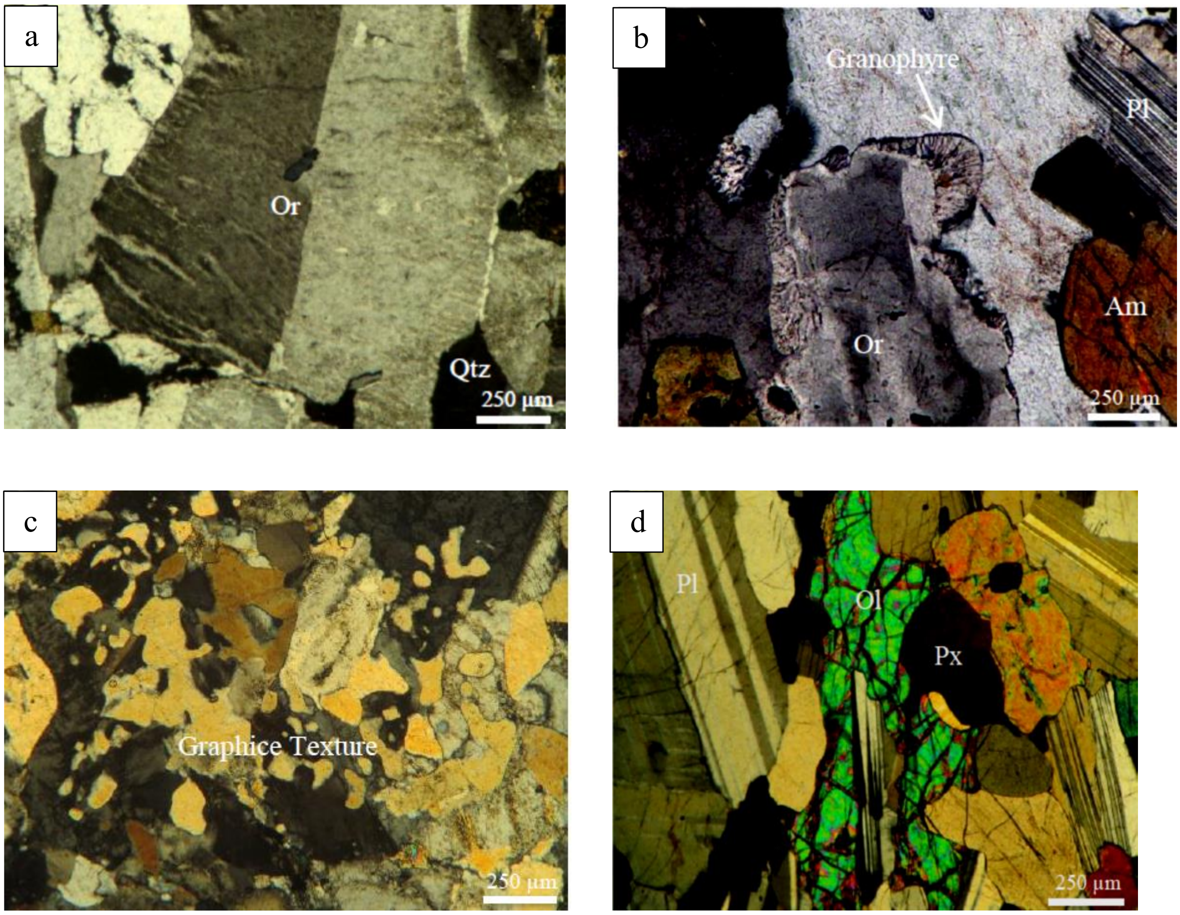

Figure 4. (*a*) perthitic texture with carlsbad twinning in granodiorite; (*b*) granophyric texture in quartz monzonite; (*c*) graphic texture in granodiorite; (*d*) poikilitic texture in olivine gabbro.
Source: Authors (2020).

SECONDARY TEXTURES

Besides the above-mentioned primary textures, secondary textures are also found in granitoid rocks and can be classified into the following three general groups (Shelley, 1993):

1. Textures appearing during cooling or late-stage metasomatism that do not result in considerable changes in the mineralogy. This group includes perthite in potassium feldspar, which is an expansion of material exchange at the potassium feldspar–myrmekitic interface. Perthitic and myrmekitic textures can be found in thin sections of local rocks;

2. Textures forming due to deuteric or hydrothermal activities and transform the primary minerals. This group includes sericitization, saussuritization, epidotization, and kaolinization alteration, which are commonly found in sections;
3. Textures indicating strain during deformation;

b.1) Perthitic Texture

The perthitic texture is a characteristic of the granites in the study region (Figure 4a). This texture is the result of the immiscibility of sodium and potassium-rich phases in alkali feldspar. Some physical and chemical factors are also effective in perthite formation. These factors include fluid pressure (such as water vapor, carbon dioxide), temperature, and the depth of magma. Parsons and Brown (1984) attribute coarser perthites to more recent hydrothermal activities at below 400 °C. However, some researchers ascribe coarse perthites to replacement activities (Smith, Brown, 1988). Furthermore, the tectonic strain may result in immiscibility, affecting the preferential orientation of perthite blades. In most coarse perthites, mutual replacement takes place in closed systems; that is, perthites coarsen without suffering a drastic transformation in the chemical composition. On the other hand, clear chemical changes take place in an open system that lead to the formation of coarse perthite in pegmatites (Martine *et al.*, 1995). The solvus line of feldspars can be used in the thermometry of perthitic rocks (Kretz, 1994). Based on the crystallization and exsolution curves of alkali feldspar, the solidification temperature of alkali feldspar (TS) in local granite rocks, at 1–2 kbar pressure, was estimated at 850–900 °C, and perthite formation temperature (Tx) at 650 °C (Figure 5).

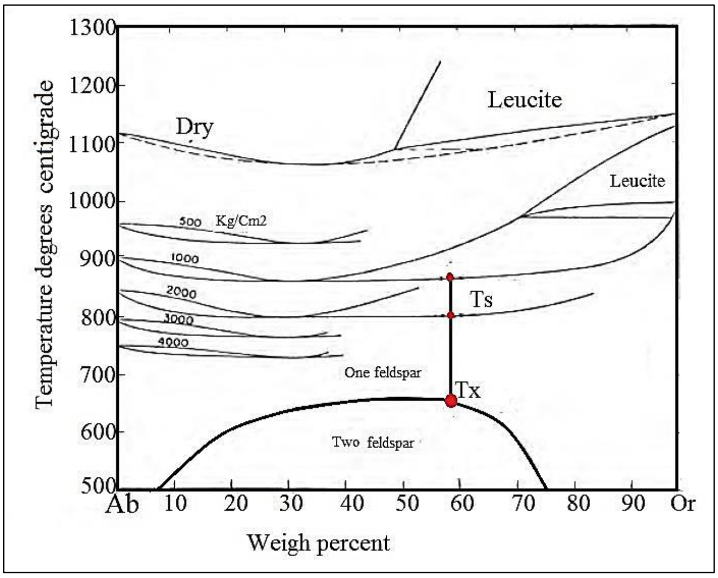

Figure 5. The binary potassium and sodium feldspar system under 1 atm dry pressure and different wet pressures.
Source: Tuttle and Bowen (1958).

b.2) Myrmekitic Texture

Myrmekitic is the branched intergrowth of quartz in plagioclase. Myrmekitics grow from grain boundaries into the grain, replacing feldspar. Accordingly, fully-crystalline plagioclase develops an onion-like appearance. Two processes have been proposed by researchers for myrmekite formation: 1. Solid-state replacement with deformation (Ahadnejad *et al.* 2011). 2. Magmatic origin. In the second case, two types of myrmekite are formed (Vernon, 1991), namely rim myrmekite, developing between potassium feldspar and plagioclase, and granular myrmekite, which resembles a bleb between adjacent potassium feldspar grains. Since it was first described by Michel Lévy (1874), myrmekite has been explained by several theories. Phillips (1974) classified these theories into six groups.

1. Simultaneous or direct crystallization: One of the oldest theories, ascribing the formation of myrmekite to the simultaneous crystallization of quartz and plagioclase from the same melt (Spencer, 1983).

2. Plagioclase replacement by potassium feldspar: The following reactions can represent subsolidus potassium feldspar replacement.

   (orthoclase) KA1Si308+Na+ = NaAlSi308(albite) + k+

   (orthoclase) KA1Si308+Ca2+ = CaA12Si2O8 (anorthite)+ 4S2O +2k+

   The constitutes of the albite and anorthite solid solutions form sodic plagioclase and silica waste in the form of vermicular quartz. The model may explain rim myrmekite

3. Potassium feldspar replacement by plagioclase: According to this hypothesis, myrmekite is part of a reaction where plagioclase is replaced by potassium feldspar under metasomatic conditions. The replacement requires additional silica in potassium feldspar, which was used in myrmekite to replace potassium feldspar. The development of vermicular quartz in the adjacent potassium feldspar supplies the SiO2 required by the plagioclase replaced by potassium feldspar.

4. Solid-state exsolution: The hypothesis does not explain the albite-rich composition of myrmekitic plagioclase and also fails to elucidate the development of myrmekite in between plagioclase and potassium feldspar.formation but fails to do so for granular myrmekite (Phillips, 1974);

5. Inclusion of recrystallized quartz in albite exsolved from growing potassium feldspar. The hypothesis assumes the incorporation of recrystallized quartz in growing albite (Shelley, 1964). The albite exsolved from potassium feldspar grows over the plagioclase crystal nuclei, encompassing the existing rod-shaped quartz in zones crushed between plagioclase and potassium feldspar. The hypothesis was challenged by Ashworth (1972) on the basis of the molecular ratio of quartz in myrmekite.

6. Other hypotheses combining the above.

7. Formation by deformation: A recent hypothesis holds that the myrmekite formation reaction starts with a combination of stress/strain concentration and fluid intrusion during deformation. Therefore, myrmekite does not form in low-grade metasomatic

> rocks, and its outcrop is limited to average and high-grade metasomatic rocks, forming in solid-state granitoids after crystallization. The required temperature for myrmekite formation can be in the 500–650 °C range (below the solidus of granite rocks). Myrmekite cannot form in cataclastic rocks that form by deformation at lower temperatures. As mentioned by Vernon (1991), stress can be a major indirect aid to myrmekite growth by facilitating the access of fluids to drive the growth. Myrmekite systematically forms at high normal-pressure sites during shear deformation (Simpson & Wintsch, 1989). At a low fluid-to-rock ratio, myrmekite nucleation seemingly starts only by stress/strain concentration (Menegon *et al.*, 2006). Myrmekite formation can lead to permeability at the microscale, thus facilitating fluid access to reaction sites where myrmekite growth takes place.

Based on studies on the local rocks, myrmekite has magmatic origins and is mostly of the rim type, which forms by the replacement of potassium feldspar with plagioclase (Figure 6a).

b.3) Corona Texture

According to Claeson (1998), the disruption of the balance between olivine and plagioclase results sets the stage for corona formation. Corona structures are indicators of ambient physicochemical changes experienced by the rock. Overall, coronas are divided into three general groups (Lamoen, 1979):

1. Those forming by olivine–plagioclase reaction;
2. Those forming by opaque oxide–plagioclase reaction;
3. Those forming by opaque oxide–clinopyroxene reaction;

It is important to note that, in thin sections, the olivines contacting pyroxene have not reacted and have remained intact. In fact, in these sections, the corona developed only where olivine was in direct contact with plagioclase. In conclusion, local plagioclases are of the olivine–plagioclase type. The product of the reaction is a fine-grained rim formed by

Revista Geoaraguaia
ISSN:2236-9716
Barra do Garças – MT
v.10, n. esp. Geologia e Pedologia p.56-79. Dez-2020

orthopyroxene and amphibole. The following formula is the best representation of the corona formation reaction (Lang *et al.,* 2004).

$$Pl + Ol + H2O \longrightarrow Di + Amp + Spl + Opx$$

The reaction starts from crystal edges and fractures inside primary olivines. The texture composition shows that during the cool-down of the old magma or subsolidus cooling, a maximum of two corona textures can develop (Acquafredda *et al.*, 1992). Magmatic coronas are characterized by an internal orthopyroxene layer and an external layer composed of orange and brown amphibole. Subsolidus coronas are often composed of an internal, often pale, amphibole, and an external amphibole+spinel layer. The intergrowth results in a symplectic configuration. The first type is more prevalent in local coronas (Figure 6a and b).

b.4) Textures Resulting from Deuteric Alteration

Water-rich mixes that are the final products of igneous crystallization promote the alteration of previously-solidified igneous rocks. Particularly along the rim of the rock or the joints and gaps, this alteration is known as deuteric alteration (Shelley, 1993).

The sections indicated a drastic transformation of plagioclase crystals into sericite. Sericite growth requires a supply of water and K+. Therefore, the process can advance only when water-rich solutions are available. The most important source of potassium ions is the chloritization of biotite. In this case, potassium ions react with anorthite formations of the plagioclase releasing Ca2+. Therefore, anorthite-rich parts of a plagioclase are easily sericitized. Sericitization is characterized by the depletion of silicates of Ca, Mg, and Na, resulting in the replacement of aluminosilicates, particularly plagioclases, with fine-grained and fibrous (sericite) mica. This phenomenon takes place at around 300–350 °C.

Saussuritization is another secondary transformation that is found in thin sections (Figures 3 and 6c). Saussurite is another product of plagioclase alteration, during which the anorthite constituent transforms into epidote and the remaining plagioclase to albite. Saussurite forms in greenschist facies (its low-pressure equivalent) and is often accompanied by epidote, albite, calcite, and sericite. Saussurite is suggestive of the concentration of hydrothermal reaction products, in particular solutions, as epidote appears selectively in anorthite-rich parts of plagioclase.

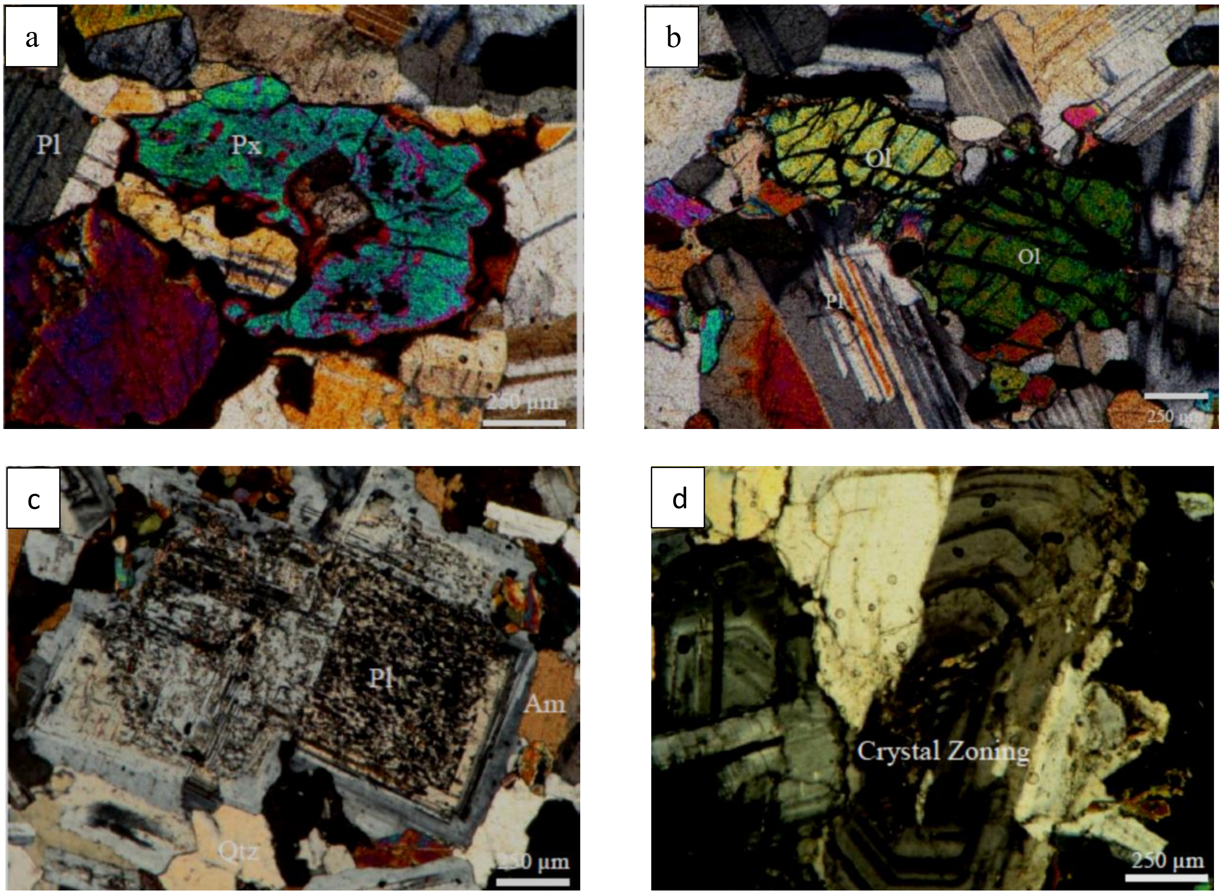

Figure 6. (*a* - *b*) corona texture in olivine gabbro; (*c*) Plagioclase decomposed into clay minerals in granodiorite; (*d*) Oscillatory zoning with alteration in plagioclase in quartz monzonite.
Source: Authors (2020).

CONCLUSION

The bulk of local rocks are made up of syenogranite, monzogranite, granodiorite, quartz monzonite, quartz monzodiorite, and olivine gabbro. The primary minerals of the local granitoids are orthoclase, plagioclase, quartz, and, to some extent, hornblende and biotite. Further, apatite, zirconia, and primary sphene were also found as accessory minerals in these rocks. Local granitoid rocks feature granular, granophyric, graphic, perthitic, and myrmekitic textures.

The granophyric texture is suggestive of the shallow depth, and the perthitic texture indicates hypersolvus conditions during the formation of the granite.

The granophyric texture of local rocks, lack of a metasomatic aureole between plutonic rocks and the surrounding igneous rocks, presence of pegmatite, and lack of primary biotite are all signs of the shallow depth of the plutonic rocks and the high water vapor pressure. Based on the texture type and the approximate temperature (850–900 °C), the rocks have replaced a water-rich magma at shallow depth. Coronas in the gabbros are of the olivine–plagioclase type. Corona formation has a direct relationship with the temperature and water supply and the migration of ions and is of magmatic type.

REFERENCES

ACQUAFREDDA, P.; CAGGIANELLI, A.; PICCARRETA, G. Late magmatic to subsolidus coronas in gabbroic rocks from the silamassif (Calberiya, Italy). **Mineralogy and Petrology**, Springer Wien, 46 (3), 1992. p. 229- 238.

AHADNEJAD, V.; VALIZADEH, M. V.; DEEVSALAR, R.; REZAEI-KAHKHAEI, M. Age and geotectonic position of the Malayer granitoids: Implication for plutonism in the Sanandaj-Sirjan Zone, W Iran. **NeuesJahrbuchfürGeologie und Paläontologie, Abhandlungen**, 261(1), 2011. p. 61-75.

ASHRAFI, N.; HASEBE, N.; JAHANGIRI, A. Cooling history and exhumation of the Nepheline Syenites, NW Iran: Constraints from Apatite fission track, **Iranian Journal of Earth Sciences**, 10(2), 2018. p. 109-120.

ASHWORTH, J.R Myrmekite of exsolution and replacement origins. **Geological Magazine**, 109, 1972. p. 45–62.

BARATIAN, M.; ARIAN, M. A.; YAZDI, A. Petrology and petrogenesis of the Siah Kuh intrusive Massive in the South of Khosh Yeilagh. **Amazonia Investiga**, 7(7), 2018. p. 616-629.

BARKER, D. S. Composition of granophyre, myrmekite and graphic granite. **Geological Society of America**, **Bulletin**, v. 81, 1970. p. 3339-3350.

BEST, M. G.; CHRISTIANSEN, E. H. **Igneous Petrology**. Oxford: Black well 2001.

BLENKINSOP, T. G **Deformation microstructures and mechanisms in minerals and rocks**. Kluwer Academic Publishers: Dordrecht, 2000.

BLUNDY, J.; CASHMAN, K. Rapid decompression-driven crystallization recorded by melt inclusions from Mount St. Helens Volcano. **Geology**, Vol. 33 (10), 2005. p. 793-796.

BOUCHEZ, J.L.; DELAS, C.; GLEIZES, G.; NÉDÉLÉC, A., CUNEY M Submagmatic microfractures in granites. **Geology**, 20, 1992. p. 35–38.

CLAESON, D. T. Coronas, reaction rims, symplectites and emplacement depth of Rymmen Gabbro,Transscandiavian igneous belt, southern Sweden. **Mineralogy Magazine**, 26, 1998. p. 743-757.

DABIRI, R.; AKBARI-MOGADDAM, M.; GHAFFARI, M. Geochemical evolution and petrogenesis of the eocene Kashmar granitoid rocks, NE Iran: implications for fractional crystallization and crustal contamination processes. **Iranian Journal of Earth Sciences**, 10(1) 2018. p. 68-77.

DUNHUM, A. C. The nature and origin of the groundmass textures in felsites and granophyres from Rhum, In vernessshire, Geological Magazine, 102, 1965. p. 8-23.

EGGLETON R. A. The ordering path for igneous K-feldspar megacrysts. **American Mineralogist**. 64, 1979. p. 906–911.

EGGLETON R. A.; BUSECK P. R. The orthoclase–microcline inversion: a high-resolution TEM study and strain analysis. **Contributions to Mineralogy and Petrolology**, 74, 1980. p. 123–133.

FENN, P. M Nucleation and growth of alkali feldspar from a melt. *In* MACKENZIE, W. S. & ZUSSMAN, J. (eds) **The Feldspar**. Manchester: Manchester University Press, 1974.

FITZGERALD J.G., MCLAREN A.C The microstructures of microcline from some granitic rocks and pegmatites. **Contributions to Mineralogy and Petrology**, 80, 1982. p. 219–229.

GHOLIZADEH, S.; ARIAN, M. A.; JAFARI, M. R.; YAZDI, A. Petrology of Intrusive Bodies of Azizabad-Tinamo Area in the South of Songour, Iran". **Open Journal of Geology**, 6, 2016. p. 1567-1579. <DOI: 10.4236/ojg.2016.612111>

GILE, H. A.; BONI, M.; BALSSONE, G.; ALLEN, C. R.; BANKS, D.; MOORE, F. Marble-hosted sulfide ores in the Angouran Zn–(Pb–Ag) deposit, NW Iran: interaction of sedimentary brines with a metamorphic core complex. **Mineralium Deposita**, 41, 2006. p. 1–16.

GINIBRE, C.; KRONZ, A.; WÖRNER, G. High-resolution quantitative imaging of plagioclase composition using accumulated backscattered electron images: new constraints on oscillatory zoning. **Contributions to Mineralogy and Petrology**, Vol. 142, 2002. p. 436-448.

HOGAN, J. P.; GILBERT, M. C **The A type Mount Scott granite sheet**: Importance of Crustal Magma Traps," Journal of Geophysical Research, vol. 100, no. B8, pp. 15779-15792, Wiley-Blackwell, Aug 1995.

HUGHES, C. Anatomy of granophyre intrusions, Lithos, 4, 2003. p. 403-415.

HUMPHREYS, M. C. S.; BLUNDY, J. D.; SPARKS, S. J. Magma evolution and opensystem processes at shiveluch volcano: insights from phenocryst zoning. **Journal of Petrology**, Vol. 47 (12), 2006. p. 2303-2334.

KRETZ, R. **Metamorphic crystallization**, Wiley: Chichester, England, 1994.

LAMOEN, H. V. Coronas in Olivine and Gabbros an Ores from Susimaki and Riuttamaa, Finland. **Contributions to Mineralogy and Petrology**, 68, 1979. p. 259- 268.

LANG, H. M.; WACHTER, A.; PETERSO, V.; RYON, J. G. Coexisting clinopyroxene / spinel and amphibole / spinel symplectites in metatroctolites from the Buck Creek ultramafic body. **American Mineralogist**, 89, 2004. p. 20-30.

LOOMIS T. P. Numerical simulations of crystallization processes of plagioclase in complex melts: the origin of major and oscillatory zoning in plagioclase". **Contributions to Mineralogy and Petrology**, 81, 1982. p. 219-29.

MARTINE, R.; PARSONS, L.; PARSONS, I. Microtextural controls of weathering of perthitic alkali feldspars, **Geochimica et cosmochimica Acta**, Volume 59, Issue 21. 1995. p. 4488-4465.

MENEGON, L.; PENNACCHIONI, G.; STÜNITZ, H. Nucleation and growth of myrmekite during ductile shear deformation in metagranites. **Journal of Metamorphic Geology**, 24, 2006. p. 553-568 .

MICHEL LÉVY, A. M. Structure microscopique des roches acides anciennes, **Société Francaise de Mineralogie et de Crystallographie Bulletin**, 3, 1874. p. 201-222.

MOBASHERGERMI, M.; ZAREI SAHAMIEH, R.; AGHAZADEH, M.; AHMADIKHALAJ, A.; AHMADZADEH, G. Mineral chemistry and thermobarometry of Eocene alkaline volcanic rocks in SW Germi, NW Iran, Iranian Journal of Earth Sciences, 10(1), 2018. p. 39-51.

NAZEMI, E.; ARIAN, M. A.; JAFARIAN, A.; POURKERMANI, M.; YAZDI, A. Studying The Genesis Of Igneous Rocks In Zarin-Kamar Region (Shahrood, Northeastern Iran) By Rare Earth Elements. **Revista Gênero e Direito**, 8(4), 2019. p. 446-466. DOI: <https://doi.org/10.22478/ufpb.2179-7137.2019v8n4.48442>

NELSON, S. T.; MONTANA, A. Sieve – textured plagioclase in volcanic rocks prodused by rapid decompression. **American Mineralogist**, Vol. 77, 1992. p. 1242-1249.

NIXON G. T.; PEARCE T. H. Laserinterferometry study of oscillatoryzoning in plagioclase: the record of magma mixing and phenocryst recycling in calk-alkaline magma chambers", Iztaccihuatl volcano, Mexico. **American Mineralogist**, 72, 1987. p. 44-62.

PARSONS, I.; BROWN, W. L. Feldspars and the thermal history of igneous rocks. **Nato Advanced study institute Serices C**, 137, 1984. p. 317-71.

PASSCHIER, C. W.; TROUW, R. A. J. **Microtectonics**. Springer-Verlag: Berlin Heidelberg, 2005.

PASSCHIER, C. W., TROUW, R. A. J. **Microtectonics**. Springer-Verlag: New York, 1998.

PATERSON, S. R.; VERNON, R. H.; TOBISCH, O. T. A review of criteria for the of magmatic and tectonic foliations in granitoids. **Journal of Structural Geology**, 11, 1989. p. 349-364.

PHILLIPS, E. R. Myrmekite-one hundred years later, **Lithos** 7, 1974. p. 181-194.

SHELLEY, D On myrmekite, **American Mineralogist**, 49, 1964. p. 41–52.

SHELLY, D **Igneous and metamorphic rocks under microscope classification features, microstructures and mineral preferred orientations**. Chapman & Hall: London., 1993.

SIMPSON, C.; WINTSCH, R. P. Evidence for deformation-induced K-feldspar replacement by myrmekite. **Journal of Metamorphic Geology**, 7, 1989. p. 261–275.

SINGER, S. B. A.; DUNGAN. M.; LAYNE, G. texture and Sr, Ba, Mg, Fe, K and Ti compositional profile in volcanic plagioclase: clues to the dynamics of calce alkaline magma chamber. **American Mineralogist**, Vol. 80, 1995. p. 776-798.

SMITH, J. V.; BROWN, W. L. **Feldspars minerals**, 2nd end, Vol. 1, springer-Verlag, Berlin. 1988.

SMITH, J. V. **Feldspar minerals, chemical and textural properties**. Springer-Verlag, vol. 2, New York, 1974

SPENCER, E. The potash-soda-feldspars. II. Some applications to petrogenesis, **Mineralogical Magazine**, 25, 1938. p. 87–118.

STEWART, M. L.; PEARCE, T. H. Sieve-textured plagioclase in dacitic magma: Interference imaging results. **American Mineralogist**, 89, 2004. p. 348-351.

TARABI, S.; EMAMI, M. H.; MODABBERI, S.; SHEIKH ZAKARIAEE, S. J. Eocene-Oligocene volcanic units of momen abad, east of Iran: petrogenesis and magmatic evolution. **Iranian Journal of Earth Sciences**, 11(2), 2019. p. 126-140.

TSUCHIYAMA, A. Dissolution kinetics of plagioclase in melt of the system diopsidealbiteanorthite,and the origin of dusty plagioclase in andesites. **Contributions to Mineralogy and Petrology**, Vol. 89, 1985. p. 1-16.

TUTTLE, O. F.; BOWEN, N. L. Origin of granite in light of experimental studies in the system NaAlSi3O8-KAlSi3O8-SiO2-H2O. Geological Society of America Memoir, 74, 1958. p. 88-96.

VERNON, R. H. Questions about myrmekite in deformed rocks. **Journal of Structural Geology**, 13, 1991. p. 979-985.

VERNON, R. H. Review of microstrucrtural evidence of magmatic and solid-state flow, **Electronic Geosciences**, 5 (2), 2000. p. 1–23.

VERNON, R. H. **A practical guide to rock microstructure**. Cambridge University Press: Cambridge, 2004.

VOGT, T. On the chronological order of deposition of the Highland schists. **Geological Magazine**, 67, 1930. p. 68–73.

YAZDI, A.; ASHJA ARDALAN, A.; EMAMI, M. H.; DABIRI, R.; FOUDAZI, M. Magmatic interactions as recorded in plagioclase phenocrysts of quaternary volcanics in SE Bam (SE Iran). **Iranian Journal of Earth Sciences**, 11(3) 2019a. p. 215-225.

YAZDI, A.; ASHJA-ARDALAN, A.; EMAMI, M. H.; DABIRI, R.; FOUDAZI, M. Chemistry of Minerals and Geothermobarometry of Volcanic Rocks in the Region Located in Southeast of Bam, Kerman Province. **Open Journal of Geology**, 7, 2017. p. 1644-1653. DOI: <10.4236/ojg.2017.711110>

YAZDI, A.; SHAHHOSINI, E.; DABIRI, R.; & ABEDZADEH, H. Magmatic Differentiation Evidences And Source Characteristics Using Mineral Chemistry In The Torud Intrusion (Northern Iran). **Revista GeoAraguaia**, 9(2), 2019b. p. 6-21.

ZADMEHR, F.; SHAHROKHI, S. V. Separation of geochemical anomalies by concentration-area and concentration-number methods in the Saqez 1:100,000 sheet, Kurdistan, Iranian **Journal of Earth Sciences**, 11(3) 2019. p. 196-204.